THE MONOGENIC RIESZ-LAPLACE WAVELET TRANSFORM

Michael Unser, Katarina Balać, Dimitri Van De Ville

Ecole Polytechnique Fédérale de Lausanne, Biomedical Imaging Group
Station 17, CH1015, Lausanne (VD), Switzerland
phone: + (41) 21 6931185, http://bigwww.epfl.ch

ABSTRACT

We introduce a family of real and complex wavelet bases of $L_2(\mathbb{R}^2)$ that are directly linked to the Laplace and Riesz operators. The crucial point is that the family is closed with respect to the Riesz transform which maps a real basis into a complex one. We propose to use such a Riesz pair of wavelet transforms to specify a multiresolution monogenic signal analysis. This yields a representation where each wavelet index is associated with a local orientation, an amplitude and a phase. We derive a corresponding wavelet-domain method for estimating the underlying instantaneous frequency of the signal. We also provide a simple mechanism for improving the shift and rotation-invariance of the wavelet decomposition. We conclude the paper by presenting a concrete analysis example.

1. INTRODUCTION

The analytical signal is a complex extension of a 1D signal that is based upon the Hilbert transform. This representation gives access to the instantaneous amplitude and phase of a signal and is widely used in applications involving some kind of amplitude or frequency modulations. This type of AM/FM analysis can also be performed in a multiresolution framework using Kingsbury's dual-tree wavelet transform, which consists of two wavelet transforms which are (approximately) Hilbert transforms of one another [1].

The analytical wavelet approach has also been extended to higher dimensions through a proper combinations of positive and negative frequency bands, allowing for a separation into six distinct orientation channels [2]. While this constitutes a valuable achievement, this type of tensor-product extension is not entirely satisfactory from a theoretical nor conceptual point of view. In particular, it is not truly rotation-invariant since the underlying basis functions are not steerable. Another way to put it is that the 2D extension of the dual-tree wavelet transform can only perform a AM/FM analysis along certain preferential orientations.

While there have been several attempts to generalize the analytical signal to two dimensions, the most successful one to date is the monogenic signal of Felsberg and Sommer [3]. The key idea of these authors was to consider the Riesz transform as the proper multi-dimensional generalization of the 1D Hilbert transform, and to introduce a corresponding quaternion formalism.

Our goal in this paper is to specify a minimally-redundant wavelet counterpart of Felsberg's monogenic signal representation. The approach is analogous to Metikas and Olhede's construction of a monogenic continuous wavelet transform [4], with the fundamental difference that we are focusing on (non-redundant) wavelet bases. The main features of the proposed wavelet decomposition are:

- The monogenic wavelet transform has three components for any scale/location index; the mother analysis wavelet is essentially isotropic, while the two others are the components of the Riesz transform of the former. In our formulation, the two Riesz wavelets are combined into a single complex transform.
- The three wavelet components give access to the local orientation, as well as to the key AM/FM parameters in the preferred orientation: amplitude, phase, and instantaneous frequency.
- The monogenic wavelet analysis is essentially rotation-invariant because of: (1) the isotropy of the mother wavelet, and (2) the fact that the the Riesz transform is steerable.
- The wavelet transform has a fast filterbank algorithm. In fact, the decomposition involves the concatenation of two wavelet bases of $L_2(\mathbb{R}^2)$, the second of which is complex-valued.

2. COMPLEX RIESZ-LAPLACE WAVELETS

Our construction hinges on the specification of three fractional differential operators:
- the fractional Laplacian of order $\alpha \in \mathbb{R}^+$

$$(-\Delta)^{\alpha} f(\boldsymbol{x}) \quad \stackrel{\mathscr{F}}{\longleftrightarrow} \quad \|\boldsymbol{\omega}\|^{2\alpha} \hat{f}(\boldsymbol{\omega}), \tag{1}$$

- the complex version of the 2D Riesz transform,

$$\mathrm{R} f(\boldsymbol{x}) \quad \stackrel{\mathscr{F}}{\longleftrightarrow} \quad \frac{(j\omega_x - \omega_y)}{\|\boldsymbol{\omega}\|} \hat{f}(\boldsymbol{\omega}), \tag{2}$$

- and its inverse

$$\mathrm{R}^{-1} f(\boldsymbol{x}) \quad \stackrel{\mathscr{F}}{\longleftrightarrow} \quad \frac{(-j\omega_x - \omega_y)}{\|\boldsymbol{\omega}\|} \hat{f}(\boldsymbol{\omega}), \tag{3}$$

where $\hat{f}(\boldsymbol{\omega}) = \mathscr{F}\{f\}(\boldsymbol{\omega}) = (2\pi)^{-2} \int_{\mathbb{R}^2} f(\boldsymbol{x}) e^{-j\langle \boldsymbol{x}, \boldsymbol{\omega} \rangle} \mathrm{d}x \mathrm{d}y$ with $\boldsymbol{\omega} = (\omega_x, \omega_y)$ is the 2D Fourier transform of $f(\boldsymbol{x})$ with $\boldsymbol{x} = (x, y)$. Note that these operators are non-local (unless α is integer) and that their Fourier-domain definition has to be taken in the sense of distributions.

A key observation is that these operators are all steerable: this is trivially the case for the Laplacian which is isotropic, while the complex Riesz transform (or its inverse) can be rotated by an angle θ by simple multiplication with the complex number $e^{j\theta}$. Another crucial property is that the operator R is unitary from $L_2(\mathbb{R}^2)$ into itself (the space of complex-valued finite-energy functions). In other words, $\mathrm{R}^{-1} = \mathrm{R}^*$, which is the adjoint of R.

Given an admissible 2D dilation (or subsampling) matrix $\mathbf{D}$ (e.g., cartesian or quincunx), we define the following

operator-like wavelets

$$\psi_{\gamma,N}^m(\mathbf{D}^{-1}\boldsymbol{x}) = \mathrm{R}^{-N}(-\Delta)^{\gamma/2}\phi_{2\gamma}(\boldsymbol{x}+\mathbf{e}_m), \qquad (4)$$

for $N \in \mathbb{N}, \gamma \in \mathbb{R}^+$, where

$$\phi_{2\gamma}(\boldsymbol{x}) \quad \stackrel{\mathscr{F}}{\longleftrightarrow} \quad \frac{1}{1+\sum_{\boldsymbol{k}\in\mathbb{Z}^2\setminus\{\mathbf{0}\}}\left(\frac{\|\boldsymbol{\omega}\|}{\|\boldsymbol{\omega}+2\pi\boldsymbol{k}\|}\right)^{2\gamma}}$$

and where the vectors $\{\mathbf{e}_m\}_{m=1}^M$ are in the coset $\mathscr{C}\setminus\{\mathbf{e}_0=(0,0)\}$ of the subsampling matrix $\mathbf{D}$. Note that there are $M=\det(\mathbf{D})-1$ wavelets $\psi_{\gamma,N}^m(\boldsymbol{x})$ of identical shape that are simply shifted to the available coset positions. The smoothing kernel, $\phi_{2\gamma}(\boldsymbol{x})$, is symmetric and it has the property that $\phi_{2\gamma}(\boldsymbol{k}) = \delta[\boldsymbol{k}]$; in fact, it is the unique interpolating kernel within the space of polyharmonic splines of order 2γ.

Interestingly, these wavelets are equivalent (up to a proportionality factor) to the complex polyharmonic spline wavelets defined in earlier work [5, 6], even though our initial definition did not involve the Riesz transform.

For the particular case $N=0$, we recover the fractional polyharmonic spline wavelets which are extensively characterized in [7]. In the sequel, for notational convenience, we will define the polyharmonic spline wavelet generator $\psi(\boldsymbol{x}) = (-\Delta)^{\gamma/2}\phi_{2\gamma}(\mathbf{D}\boldsymbol{x})$ (scale $i=0$) and consider the wavelet basis functions $\psi_{i,\boldsymbol{k}}(\boldsymbol{x}) = |\det(\mathbf{D})|^{i/2}\,\psi(\mathbf{D}^i\boldsymbol{x}-\mathbf{D}^{-1}\boldsymbol{k})$. The corresponding wavelet subspace at resolution i is:

$$\mathscr{W}_i = \mathrm{span}\left\{\psi_{i,\boldsymbol{k}}(\boldsymbol{x})\right\}_{\boldsymbol{k}\in\mathbb{Z}^2\setminus\mathbf{D}\mathbb{Z}^2}, \qquad (5)$$

which involves placing the rescaled wavelets at the appropriate coset positions. We recall that with the present arrangement, the lattice $\mathbf{D}\mathbb{Z}^2$ is associated with the approximation space $\mathscr{V}_i$ that is spanned by polyharmonic B-spline $\beta_\gamma(\boldsymbol{x})$, which is a valid scaling functions for $\gamma > \frac{1}{2}$ [7]. We also have the direct sum decomposition property: $\mathscr{V}_{i+1} = \mathscr{W}_i \oplus \mathscr{V}_i$, which is standard in multiresolution analysis.

Based on our previous work, we can list the following remarkable properties that are satisfied by the present class of wavelet transforms.

Property 1 *(Basis of $L_2(\mathbb{R}^2)$). The polyharmonic spline wavelet $\psi(\boldsymbol{x})$ (resp., $\mathrm{R}^{-N}\psi(\boldsymbol{x})$) generates a Riesz[1] basis for W_0 (resp., $R^{-N}W_0$). Moreover, $\{\psi_{i,\boldsymbol{k}}(\boldsymbol{x})\}_{i\in\mathbb{Z},\boldsymbol{k}\in\mathbb{Z}^2\setminus\mathbf{D}\mathbb{Z}^2}$ yields a Riesz basis of $L_2(\mathbb{R}^2)$ for all $\gamma > \frac{1}{2}$ (the same is also true for $\{\mathrm{R}^{-N}\psi_{i,\boldsymbol{k}}\}$, except that the basis is complex).*

Property 2 *(Semi-orthogonality). The Riesz-Laplace wavelets are orthogonal across scales:*

$$\forall \boldsymbol{k},\boldsymbol{l}\in\mathbb{Z}^2, i\neq j, \quad \langle \mathrm{R}^{-N}\psi_{i,\boldsymbol{k}}, \mathrm{R}^{-N}\psi_{j,\boldsymbol{l}}\rangle = 0$$

Property 3 *(Operator like-behavior). The polyharmonic spline wavelet transform implements a multiscale version of the Laplace operator:*

$$\langle f, \psi(\mathbf{D}^i\cdot-\boldsymbol{x})\rangle = (-\Delta)^{\gamma/2}(f*\varphi(\mathbf{D}^i\cdot))(\boldsymbol{x})$$

where the smoothing kernel is $\varphi(\boldsymbol{x}) = \phi_{2\gamma}(\mathbf{D}\boldsymbol{x})$, while the N-Riesz-Laplace wavelet transform does the same for the N-fold Riesz transform of the input signal:

$$\begin{aligned}\langle f, \mathrm{R}^{-N}\psi(\mathbf{D}^i\cdot-\boldsymbol{x})\rangle &= \langle \mathrm{R}^N f, \psi(\mathbf{D}^i\cdot-\boldsymbol{x})\rangle \\ &= (-\Delta)^{\gamma/2}(\mathrm{R}^N f * \varphi(\mathbf{D}^i\cdot))(\boldsymbol{x})\end{aligned}$$

Property 4 *The Riesz-Laplace wavelet transform with parameters (γ,N) has approximation order γ.*

Property 5 *(Vanishing moments). The Riesz-Laplace wavelet of order γ has $\lceil\gamma\rceil$ vanishing moments.*

Property 6 *(Fast implementation). All Riesz-Laplace wavelet transforms are perfectly reversible and they have a fast filterbank implementation.*

All the above properties are well known for the polyharmonic spline wavelets ($N=0$). They do extend to the Riesz-Laplace transform as a consequence of the unitary nature of the operator R. The important point in the argumentation is that the structure of the Gram matrix (inner products between basis functions) are independent upon N.

A somewhat trickier aspect is the specification of a valid scaling function in the latter case, since the most natural candidate $\mathrm{R}^{-N}\beta_\gamma(\boldsymbol{x})$ (where $\beta_\gamma(\boldsymbol{x})$ is a polyharmonic B-spline) is not admissible (due to the singularity of R at the origin). Fortunately, there are other B-spline-like generators that are well-behaved and that do yield a stable and efficient ("à la Mallat") filterbank implementation [6]. The crucial aspect for specifying an admissible scaling function is to ensure an appropriate lowpass frequency behavior around $\boldsymbol{\omega}=\mathbf{0}$.

Finally, we note that all the proposed wavelet transforms are best implemented in the Fourier domain using an FFT-based algorithm which is remarkably fast. We are currently working on making the software available publicly.

3. MONOGENIC WAVELET ANALYSIS

Given a 2D signal $f(\boldsymbol{x}), \boldsymbol{x}\in\mathbb{R}^2$, Felsberg and Sommer define the 3-component monogenic signal

$$\mathbf{f}_\mathrm{m}(\boldsymbol{x}) = (f(\boldsymbol{x}), \mathrm{Re}(\mathrm{R}f(\boldsymbol{x})), \mathrm{Im}(\mathrm{R}f(\boldsymbol{x}))) = (q, r_1, r_2). \qquad (6)$$

The local amplitude of the signal is given by $A(\boldsymbol{x}) = \|\mathbf{f}_\mathrm{m}(\boldsymbol{x})\| = \sqrt{q^2+r_1^2+r_2^2}$, while its local orientation θ and instantaneous phase ξ are specified by the following relations:

$$q = A\cos\xi,\ r_1 = A\sin\xi\cos\theta,\ r_2 = A\sin\xi\sin\theta. \qquad (7)$$

In this work, we consider the polyharmonic spline wavelet of order γ, and use the Riesz-Laplace wavelet transform to perform the monogenic analysis of a sequence of bandpass filtered signals $(f*\psi_i)(\boldsymbol{x})$ where $\psi_i(\boldsymbol{x}) = |\det(\mathbf{D})|^{i/2}\,\psi(\mathbf{D}^i\boldsymbol{x})$ is the normalized and rescaled wavelet a scale i. Indeed, since the analysis wavelet $\psi_i(\boldsymbol{x})$ is symmetric, we have that

$$w_i[\boldsymbol{k}] = \langle f, \psi_{i,\boldsymbol{k}}\rangle = (\psi_i * f)(\boldsymbol{x})|_{\boldsymbol{x}=\mathbf{D}^{-i-1}\boldsymbol{k}} \qquad (8)$$

$$w_i^R[\boldsymbol{k}] = \langle f, \mathrm{R}^{-1}\psi_{i,\boldsymbol{k}}\rangle = \langle \mathrm{R}f, \psi_{i,\boldsymbol{k}}\rangle \qquad (9)$$

$$= (\mathrm{R}(\psi_i * f))(\boldsymbol{x})|_{\boldsymbol{x}=\mathbf{D}^{-i-1}\boldsymbol{k}} \qquad (10)$$

[1] A Riesz basis is a fundamental concept in functional analysis that was introduced by the Hungarian mathematician Frigyes Riesz; it has not much to do with the Riesz transform that is due to Marcel Riesz (Frigyes' younger brother), except perhaps that our *complex* version of the Riesz transform maps a Riesz basis into another one.

where we have used the property $\mathrm{R}^{-1} = \mathrm{R}^*$. This means that we can perform a full multiresolution monogenic signal analysis by running two wavelet transforms in parallel. Specifically, we set the transform parameters to $(\gamma, 0)$ for extracting the real-valued signal component, and to $(\gamma, 1)$ for obtaining the corresponding complex-valued Riesz transform component.

The local signal amplitude (AM component) at scale i and location $\boldsymbol{k}$ is then given by

$$A_i[\boldsymbol{k}] = \sqrt{w_i^2[\boldsymbol{k}] + |w_i^R[\boldsymbol{k}]|^2}$$

while the corresponding local orientation is

$$\theta_i[\boldsymbol{k}] = \arctan\left(\frac{\mathrm{Im}(w_i^R[\boldsymbol{k}])}{\mathrm{Re}(w_i^R[\boldsymbol{k}])}\right),$$

Alternatively, the orientation may be represented by a unit vector $\boldsymbol{u}$. The intuitive interpretation of $\boldsymbol{u}$ is akin to the direction of the gradient; that is, the direction where the rate of change is maximal.

Once $A_i[\boldsymbol{k}]$ and $\theta_i[\boldsymbol{k}]$ have been determined, we can refer to (7) to obtain the corresponding local phase $\xi_i[\boldsymbol{k}]$. Of even greater interest is the local frequency (or wave number) that corresponds to the derivative of ξ in the direction specified by $\boldsymbol{u}$ [8]. After some algebraic manipulation (cf. Appendix), we obtain the following equation for the instantaneous frequency

$$\nu_i[\boldsymbol{k}] = \frac{\mathrm{Re}\left(w_i^R[\boldsymbol{k}]\langle f, \mathrm{R}\psi'_{i,\boldsymbol{k}}\rangle\right) - w_i[\boldsymbol{k}]\langle f, \psi'_{i,\boldsymbol{k}}\rangle}{A_i^2[\boldsymbol{k}]}, \qquad (11)$$

which has the advantage of avoiding the use of the arctan function and all the problems associated with phase-wrapping. The additional information that is required is the computation of spatial derivatives in the direction of $\boldsymbol{u}$ which is achieved economically by considering two auxiliary Riesz-Laplace wavelets ψ' and $\mathrm{R}\psi'$ of reduced order $\gamma - 1$. The definition of these auxiliary wavelets is

$$\psi'(\boldsymbol{x}) = \left(\frac{\partial}{\partial x} + j\frac{\partial}{\partial y}\right)\mathrm{R}^*\psi(\boldsymbol{x}) = (-\Delta)^{1/2}\psi(\boldsymbol{x}) \quad \overset{\mathscr{F}}{\longleftrightarrow} \quad \|\boldsymbol{\omega}\|\hat{\psi}(\boldsymbol{\omega}),$$

$$\mathrm{R}\psi'(\boldsymbol{x}) = \left(\frac{\partial}{\partial x} + j\frac{\partial}{\partial y}\right)\psi(\boldsymbol{x}) \quad \overset{\mathscr{F}}{\longleftrightarrow} \quad (j\omega_x - \omega_y)\hat{\psi}(\boldsymbol{\omega}).$$

The first is real, symmetric and is designed to calculate the "Laplacian" term $-(r_{1x} + r_{2y})$, while the second is complex and is associated with the adjoint-gradient term $(-q_x + jq_y)$ (cf. Appendix). The main point is that these additional "derivative" wavelet transforms can be calculated using essentially the same filterbank algorithm with an appropriate modification of the analysis filters. This means that the cost for obtaining an instantaneous frequency estimate is about twice that of the original monogenic wavelet decomposition. The advantage of the present formulation is that the frequency formula (11) is exact and that it does not involve any finite difference approximation of the spatial derivatives.

4. RESULTS

We will now discuss some practical issues and present concrete analysis examples. For now on, we consider the case of a dyadic analysis with $\mathbf{D} = \begin{pmatrix} 2 & 0 \\ 0 & 2 \end{pmatrix}$.

4.1 Improving the invariance properties

The monogenic wavelet transform that was introduced so far is elegant mathematically because it is tied to a basis. However, there is also a downside which is some lack of invariance. We will now show how to bypass this limitation.

4.1.1 Shift invariance

Eventhough it is build around a single wavelet, the wavelet analysis of Section 3 is somewhat awkward to interpret because the transform is missing the wavelets at the subsampling location corresponding to the next coarser grid (coset vector $\mathbf{e}_0 = (0,0)$). It is therefore tempting to include the "missing" shifts as well, and to rearrange the wavelet coefficients into a single, image-like subband at scale i. This is equivalent to *not* subsampling the wavelet subband after digital filtering. Consequently, we obtain the enlarged analysis spaces

$$\mathscr{W}_i^+ = \mathrm{span}\left\{2^i\psi(2^i\boldsymbol{x} - \boldsymbol{k}/2)\right\}_{\boldsymbol{k}\in\mathbb{Z}^2}. \qquad (12)$$

where ψ is the mother wavelet of order γ. The corresponding notation for the (non-subsampled) wavelet coefficients at scale i is $w_i[\mathbf{k}]$ (as before) and all previous formulas are still applicable with $\boldsymbol{k}$ spanning over $\mathbb{Z}^2$ instead of $\mathbb{Z}^2\backslash 2\mathbb{Z}^2$. The same arrangement is also used for the Riesz branch of the transform. This extension improves the shift-invariance of the decomposition and its cost is moderate (redundancy factor of 1/4).

4.1.2 Rotation invariance and steerability

The other weak point is that the smoothing kernel $\phi_{2\gamma}$ of our defining wavelet is not isotropic. In fact, it is sinc-like since it is an interpolating function. We propose to exploit the degrees of freedom provided by the enlarged wavelet spaces $\mathscr{W}_i^+$ to tune the kernel's shape to make the wavelet more nearly isotropic. Our solution is to select the "isotropic" polyharmonic B-spline $\beta_{2\gamma}$ as our new smoothing kernel. This is justified by the fact that this B-spline spans the same spline space as $\phi_{2\gamma}$, with the advantage that is is better localized and that it converges to a Gaussian as γ increases [7]. The frequency-domain formula for our new smoothing kernel is

$$\beta_{2\gamma}(\boldsymbol{x}) \quad \overset{\mathscr{F}}{\longleftrightarrow} \quad \left(\frac{V(e^{j\boldsymbol{\omega}})}{\|\boldsymbol{\omega}\|}\right)^{2\gamma},$$

where $V(e^{j\boldsymbol{\omega}})$ is the "most-isotropic" discrete Laplacian filter

$$V(e^{j\boldsymbol{\omega}}) = \frac{8}{3}\left(\sin^2\left(\frac{\omega_1}{2}\right) + \sin^2\left(\frac{\omega_2}{2}\right)\right) + \frac{2}{3}\left(\sin^2\left(\frac{\omega_1+\omega_2}{2}\right) + \sin^2\left(\frac{\omega_1-\omega_2}{2}\right)\right).$$

The corresponding mother wavelet to be used in replacement of the preceding one is $\psi(\boldsymbol{x}/2) = (-\Delta)^{\gamma/2}\beta_{2\gamma}(\boldsymbol{x})$, while the whole monogenic analysis procedure remains the same as described earlier. This is entirely justifiable mathematically

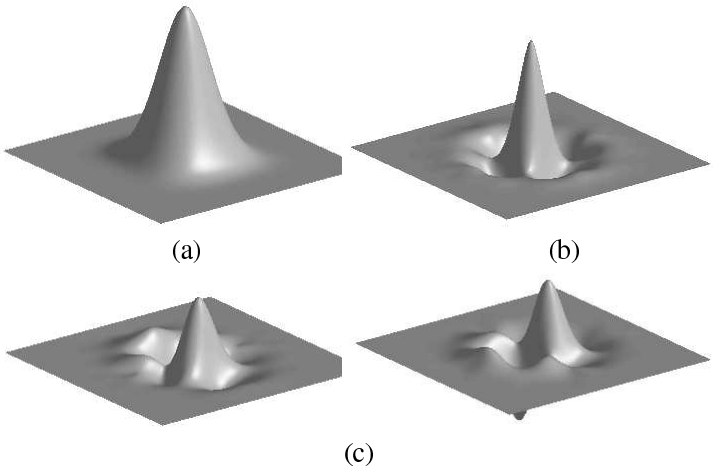

Figure 1: (a) Smoothing kernel $\beta_8(\boldsymbol{x})$. (b) Isotropic polyharmonic wavelet $\psi(\boldsymbol{x}/2) = \Delta^2\beta_8(\boldsymbol{x})$. (c) 2D Riesz transform $\mathrm{R}\psi$ of (b), real and imaginary parts.

since the modified Mexican-hat-like wavelet also spans the analysis spaces $\mathscr{W}_i^+$. Concretely, this wavelet substitution amounts to a simple change of wavelet filters in the algorithm in a manner that is fully reversible and transparent to the user. The benefit of this adaptation is a substantial improvement of the steerability of the transform; this is essential for the feature extraction process to be truly rotation-invariant.

In Fig. 1, we show the various functions for the case $\gamma = 4$. In (a), we depict the smoothing kernel β_8, which closely resembles a Gaussian with standard deviation $\sqrt{2/3}$. In (b), we show the isotropic polyharmonic mother wavelet $\psi(\boldsymbol{x}/2) = \Delta^2\beta_8(\boldsymbol{x})$. Finally, in (c), we included both the real and imaginary parts of the complex version of the 2D Riesz transform $\mathrm{R}\psi$.

4.2 Experimental result

We show an example of the monogenic wavelet analysis of the AM-encoded image. The original information image is shown in Fig. 2 (a), and its interferometric version in (b). The encoding is done by a zoneplate; i.e., a circular wave propagating with constant frequency.

The various components of the monogenic wavelet analysis are shown in Fig. 3. In (a), the directional information is adequately captured by the orientation. In (b), the instantaneous frequency is also well recovered and constant. Finally, the AM-encoded information can be retrieved by the modulus in (c). The multiscale interpretation shows the strongest signal in the second subband, since the zoneplate frequency has the highest response at this scale. The attenuation is clearly visible at the third subband. Note that the instanteneous frequency can provide more fine-granular information about the carrier wave.

5. CONCLUSION

We have set the mathematical foundations of a monogenic wavelet transform that gives access to the local orientation, amplitude and phase information of a 2D signal. The transform is build around the monogenic extension of a polyharmonic spline wavelet basis of $L_2(\mathbb{R}^2)$. The decomposition is reasonably fast, moderately redundant (a factor between 3 and 4), and fully reversible. Potential applications include various type of image analyses—in particular, interferograms—as well as image enhancement and denoising since the transform is reversible.

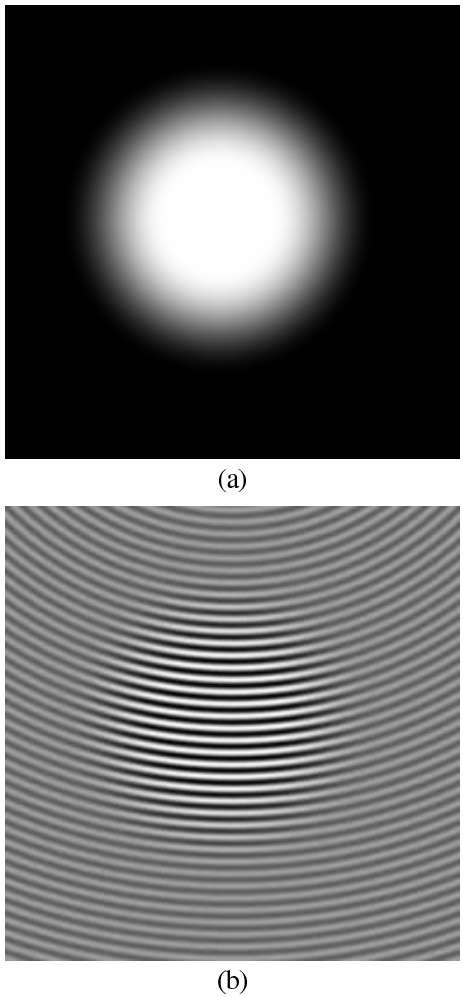

Figure 2: (a) Original information image. (b) AM-encoded interferometric version.

A. INSTANTANEOUS FREQUENCY CALCULATION

We consider the monogenic wavelet components ($q = A\cos\xi, r_1 = A\sin\xi\cos\theta, r_2 = A\sin\xi\sin\theta$) and define $r = \sqrt{r_1^2 + r_2^2} = A\sin\xi$. The orientation vector is given by $\boldsymbol{u} = (\cos\theta, \sin\theta) = (r_1/r, r_2/r)$. We also introduce the complex variable $z = Ae^{j\xi} = q + jr$, which conveniently summarizes the amplitude and phase information.

Our goal is to determine the instantaneous frequency $\nu = \mathrm{D}_{\boldsymbol{u}}\xi$, which is the derivative of ξ is the direction specified by $\boldsymbol{u}$. To that end, we first evaluate the phase gradient using the property that $\xi = \mathrm{Im}(\log z)$:

$$\nabla\xi = \mathrm{Im}\left(\frac{\nabla z}{z}\right) \quad = \quad \frac{-r\nabla q}{A^2} + \frac{q(r_1\nabla r_1 + r_2\nabla r_2)}{rA^2}$$

with the differential notation $\nabla f = (\frac{\partial f}{\partial x}, \frac{\partial f}{\partial y}) = (f_x, f_y)$. To

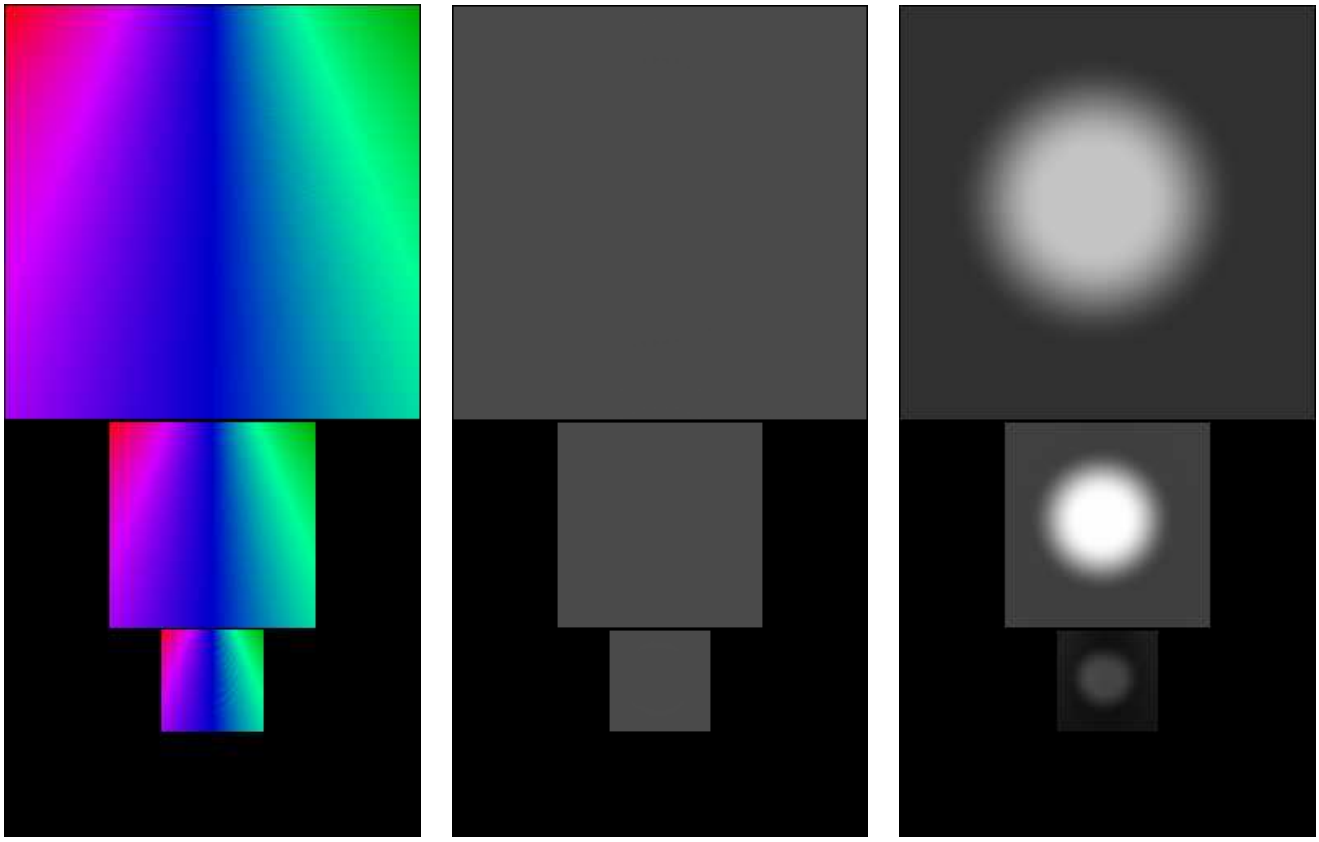

(a) (b) (c)

Figure 3: Various components of the monogenic Riesz-Laplace wavelet transform for the test image of Fig. 2 (b). (a) Orientation (in hue). (b) Instantaneous frequency. (c) Modulus.

evaluate the directional derivative, we compute the inner product with $\boldsymbol{u}$, which gives

$$\mathrm{D}_{\boldsymbol{u}}\xi = \langle \nabla\xi, \boldsymbol{u} \rangle \quad = \quad \frac{-r_1 q_x - r_2 q_y}{A^2} + \frac{q(\boldsymbol{u}^T \mathbf{H} \boldsymbol{u})}{A^2}$$

where $\mathbf{H} = \begin{pmatrix} r_{1x} & r_{1y} \\ r_{2x} & r_{2y} \end{pmatrix}$ is a symmetric matrix (analogous to the Hessian) due to the properties of the Riesz transform. If we now assume that the underlying signal is a pure plane wave that propagates in the direction $\boldsymbol{u}$, then $\mathbf{H}$ is of rank 1 and $\boldsymbol{u}^T \mathbf{H} \boldsymbol{u} = \lambda_{\max} = \mathrm{trace}(\mathbf{H}) = r_{1x} + r_{2y}$. This leads to the simplified formula

$$\nu = \mathrm{D}_{\boldsymbol{u}}\xi = \frac{-r_1 q_x - r_2 q_y}{A^2} + \frac{q(r_{1x} + r_{2y})}{A^2},$$

which is the same result as [8, Theorem 4]. The critical ingredient for this determination is to provide a numerical procedure for computing the derived quantities $(-q_x + jq_y)$ and $-(r_{1x} + r_{2y})$, which can be done in an efficient way using two reduced-order wavelet transforms, as specified in the text.

Acknowledgements

This work was supported by the Swiss National Science Foundation (MU, KB) under Grant 200020-109415 and by the Center for Biomedical Imaging (DVDV) of the Geneva-Lausanne Universities and the EPFL, as well as the foundations Leenaards and Louis-Jeantet.

REFERENCES

[1] N. Kingsbury, "Image processing with complex wavelets," *Philos. Trans. Royal Soc. London: Series A—Math. Phys. Eng. Sci.*, vol. 357, no. 1760, pp. 2543–2560, 1999.

[2] I. W. Selesnick, R. G. Baraniuk, and N. C. Kingsbury, "The dual-tree complex wavelet transform," *IEEE Sig. Proc. Magazine*, vol. 22, no. 6, pp. 123–151, 2005.

[3] M. Felsberg and G. Sommer, "The monogenic signal," *IEEE Trans. Signal Processing*, vol. 49, no. 12, pp. 3136–3144, 2001.

[4] G. Metikas and S. C. Olhede, "Multiple multidimensional morse wavelets," *IEEE Trans. Signal Processing*, vol. 55, no. 3, pp. 921–936, 2007.

[5] B. Forster, T. Blu, D. Van De Ville, and M. Unser, "Shift-invariant spaces from rotation-covariant functions," *Applied and Computational Harmonic Analysis*, in press.

[6] D. Van De Ville and M. Unser, "Complex wavelet bases, steerability, and the Marr-like pyramid," *IEEE Trans. Image Processing*, submitted.

[7] D. Van De Ville, T. Blu, and M. Unser, "Isotropic polyharmonic B-Splines: Scaling functions and wavelets," *IEEE Trans. Image Processing*, vol. 14, no. 11, pp. 1798–1813, November 2005.

[8] M. Felsberg and G. Sommer, "The monogenic scale-space: A unifying approach to phase-based image processing in scale-space," *J. Math. Imaging and Vision*, vol. 21, no. 1, pp. 5–26, 2004.